

~~RESTRICTED~~

Department of the Navy
Bureau of Ordnance
Contract NOrd 9612

FORCES ON A CYLINDER
FLANING IN A VAPOR CAVITY

R. W. Kermeen

Hydrodynamics Laboratory
California Institute of Technology
Pasadena, California

Report No. E-12.14
November, 1953

J. T. McGraw
Project Supervisor

~~RESTRICTED~~

CONTENTS

	<u>Page</u>
Abstract	
Introduction	1
Experimental Procedure	1
Definition of Terms	2
Results	4
Discussion of Results	9
Spray and Cylinder Cavitation	11
The Vapor Cavity	12
Appendix	17
A. Froude and Reynolds Number Effects on Force Measurements	
B. Data Reduction	
References	21

Abstract

The results of an experimental program carried out in the High Speed Water Tunnel to measure the forces on a cylinder planing on the inside surface of a vapor cavity are presented. Curves of lift, drag, and pitching moment coefficients and position of the center of pressure of the planing cylinder are given as functions of planing angle and draught. A brief description of the vapor cavity, spray configurations, and cylinder cavitation are included.

Introduction

A study of the trajectory of a missile running in a cavity requires knowledge of the hydrodynamic forces acting on it. For any proposed missile these forces and moments would best be measured directly for the entire vehicle. However, valuable information can be obtained by model studies of the forces on individual body components using basic geometric shapes.

Experiments have been carried out in towing tanks and in the Free Surface Water Tunnel to determine the forces on bodies planing on flat water surfaces.^{1, 2} The purpose of these tests was to obtain data applicable for the design of cavity-running missiles and to provide information on the forces exerted on a missile afterbody when it comes into contact with a cavity wall. Planing tests carried out on a flat surface give a first approximation to the actual case of a missile tail planing on a doubly curved cavity wall. A second approximation is obtained in the tests in the High Speed Water Tunnel where the planing surface is the wall of a vapor cavity. A cylinder was chosen for the planing body in these initial tests since its shape closely resembles that of the afterbody of cavity-running projectiles, and furthermore the California Institute of Technology Free Surface Water Tunnel results show that the lift forces on this shape compare closely with forces on conical afterbodies of different angles of flare.

Experimental Procedure.

The planing surface, a vapor cavity approximately 2 in. in diameter, was produced behind a 1/2-in. diameter circular disk. The disk was mounted on the spindle shield which was attached to the working section wall. A solid 1-in. diameter right circular cylinder with its axis horizontal was attached to the balance spindle. The spindle and cylinder could be yawed in a horizontal plane to any angle up to ± 22 degrees without stopping the tunnel or interrupting the run. A single large pressure tap three inches behind the disk was used to measure the cavity pressure. The water which tends to flow up the leading edge of a shield into a cavity was deflected and led aft by a thin splitter plate attached to the top of the shield. Figure 1 shows a side view of this setup.

The force measurements, lift, drag, and moment, were made by first producing a vapor cavity behind the disk with a reduction of the working section pressure at constant velocity and then yawing the cylinder until it intersected

the surface of the cavity. During each run the velocity and cavitation number were held constant and the planing angle and submergence were varied by increasing the angle of yaw of the cylinder. The planing angle and submergence were also varied by changing the length of the cylinder.

The runs covered a range of planing angles from 4 to 13 degrees with submergences up to 1.2 cylinder diameters. The planing angle and submergence were recorded photographically with a camera mounted above the working section. The photographs were taken with an exposure time of 1/25 second, which gives a smooth average cavity image. Figure 2 shows a series of photographs taken at various angles and depths during one run.

Definition of Terms

All results are presented on a nondimensional basis. Coefficients of lift, drag, and pitching moment are defined by:

$$\text{Lift coefficient } C_L = \frac{\text{lift}}{1/2 \rho V^2 d^2}$$

$$\text{Drag coefficient } C_D = \frac{\text{drag}}{1/2 \rho V^2 d^2}$$

$$\text{Pitching moment coefficient } C_M = \frac{\text{pitching moment}}{1/2 \rho V^2 d^3}$$

where

ρ = density of water in slugs/cu ft

V = velocity in ft/sec

d = diameter of cylinder in ft

The pitching moment is given about an axis through the center of the aft circular surface of the planing cylinder, point A, Fig. 3. The draught or submergence, presented as a dimensionless parameter δ/d , is defined as the distance from the original undisturbed cavity surface to the point of maximum penetration of the cylinder. The planing angle α is the angle between the undisturbed cavity wall and the edge of the cylinder. The position of the center of pressure is defined as the distance from the aft surface along the cylinder axis, and is given as L_1/d . The sketch, Fig. 3, further defines these quantities.

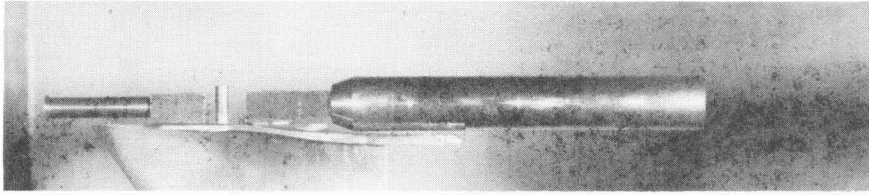


Fig. 1 - Side view of setup in working section

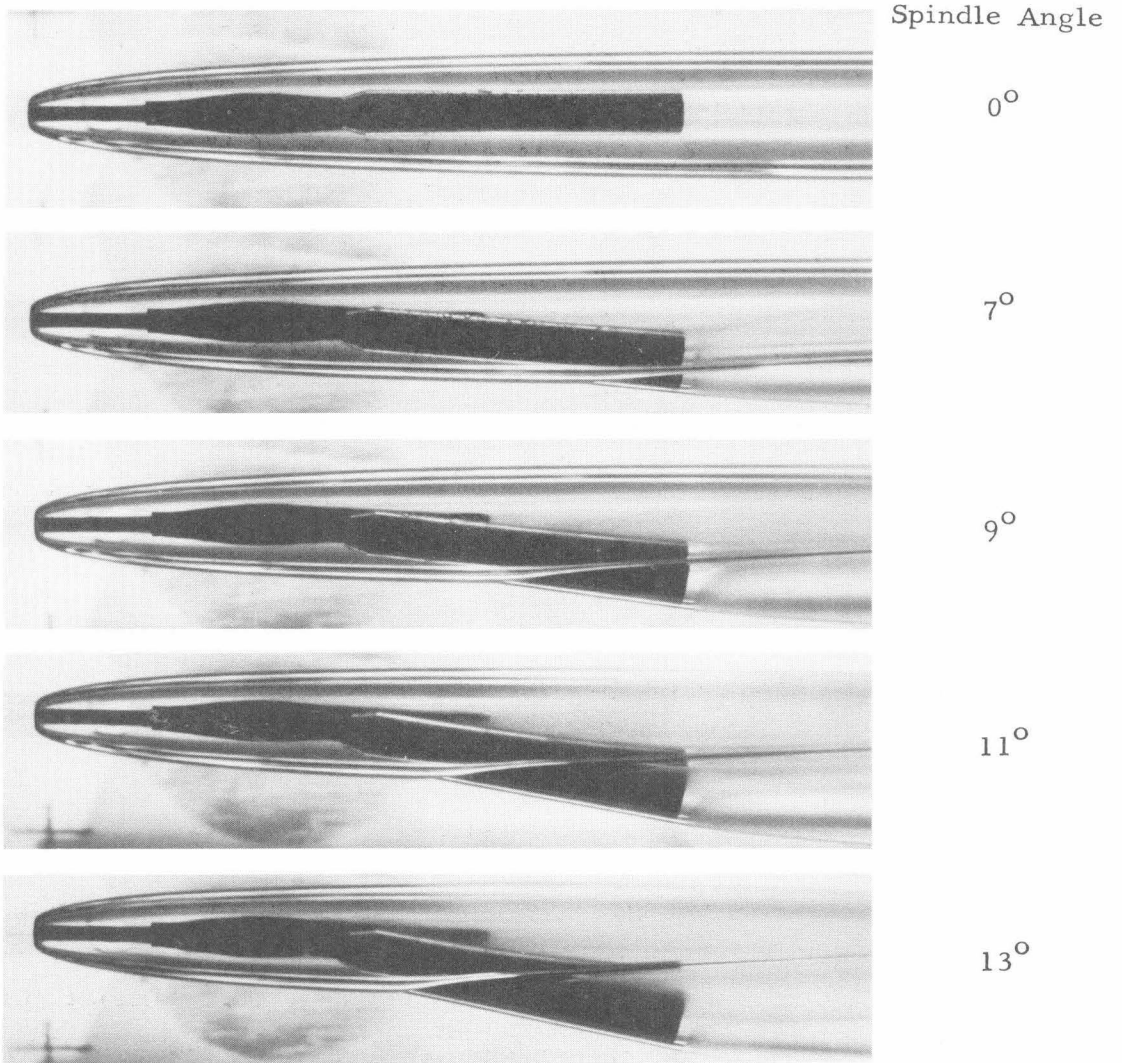


Fig. 2 - Top view of 1-in. cylinder planing in vapor cavity wall

The cavitation number is defined as

$$K = \frac{P_o - P_K}{\rho/2 V^2}$$

where

P_o is the working section pressure in lb/sq ft

P_K is the measured cavity pressure in lb/sq ft

ρ and V are as defined above.

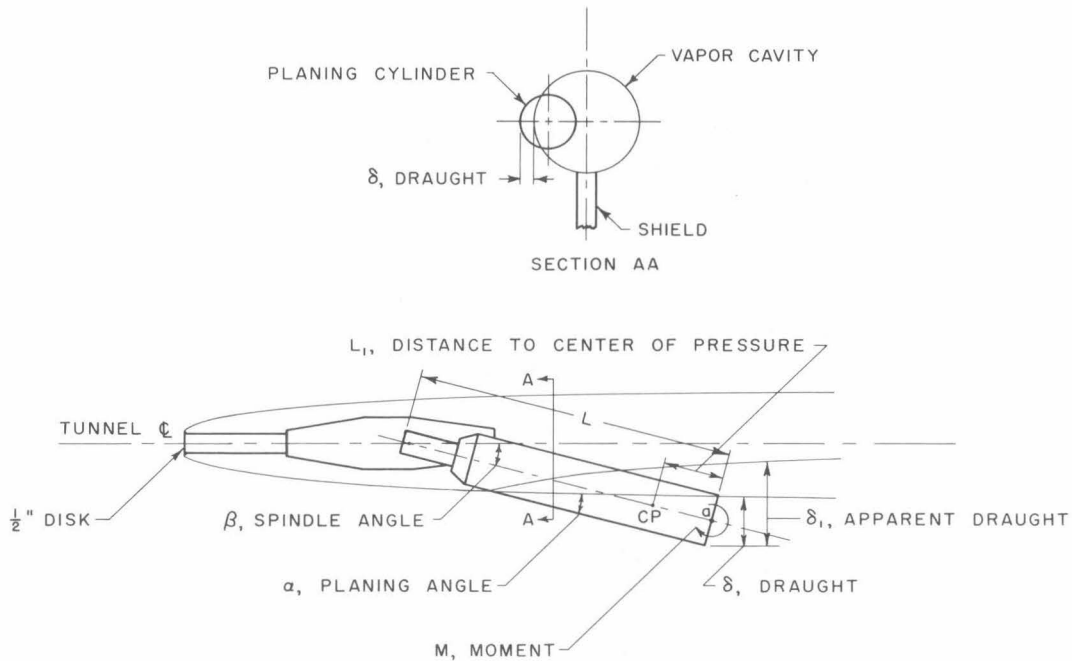


Fig. 3 - Sketches defining terms and showing relative size of vapor cavity and planing cylinder

Results

Curves of lift coefficients vs. submergences for various planing angles are shown in Fig. 4. These results have been cross plotted with lift coefficient as a function of planing angle at various draughts, Fig. 5. Similar curves for drag coefficients are shown in Figs. 6 and 7; for pitching moment, Figs. 8 and 9; for distance to center of pressure, Figs. 10 and 11.

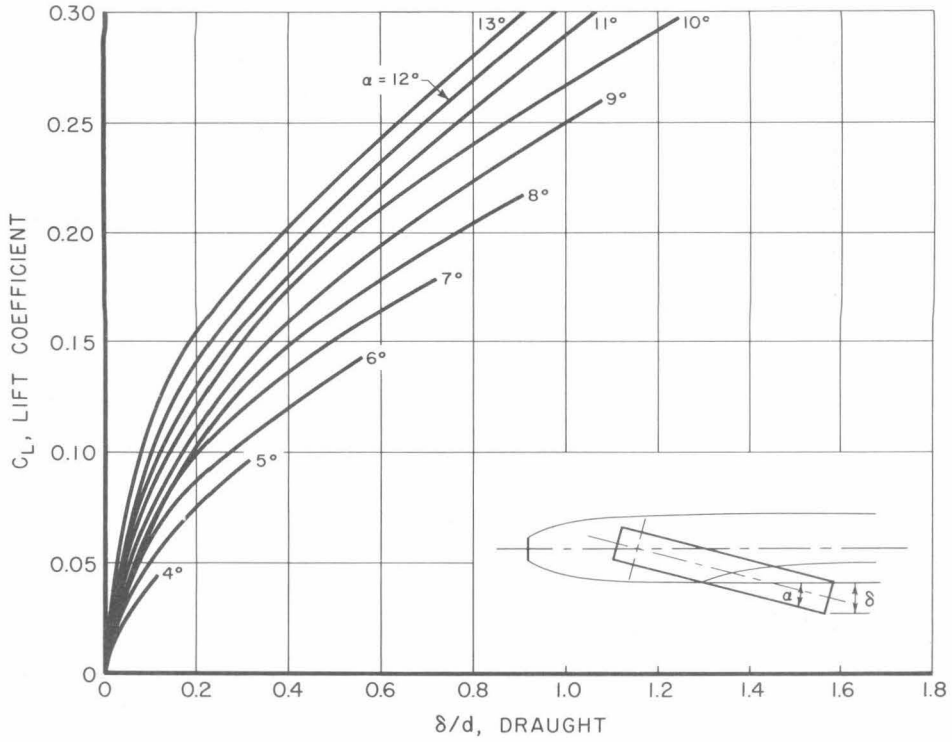


Fig. 4 - Lift coefficient vs. draught at several planing angles

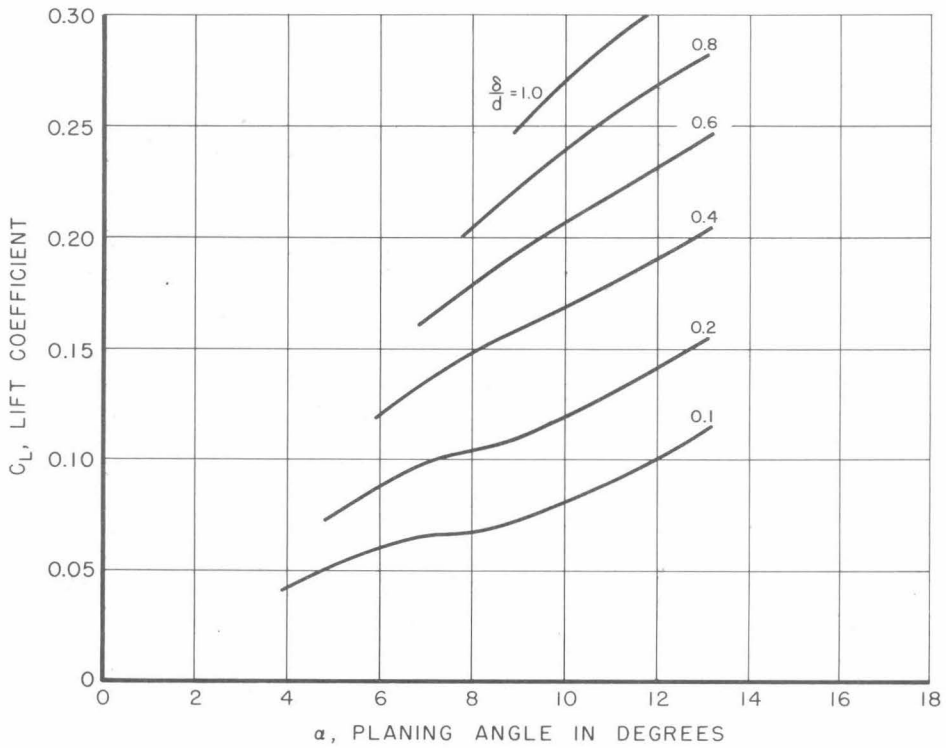


Fig. 5 - Lift coefficient vs. planing angle at several draughts

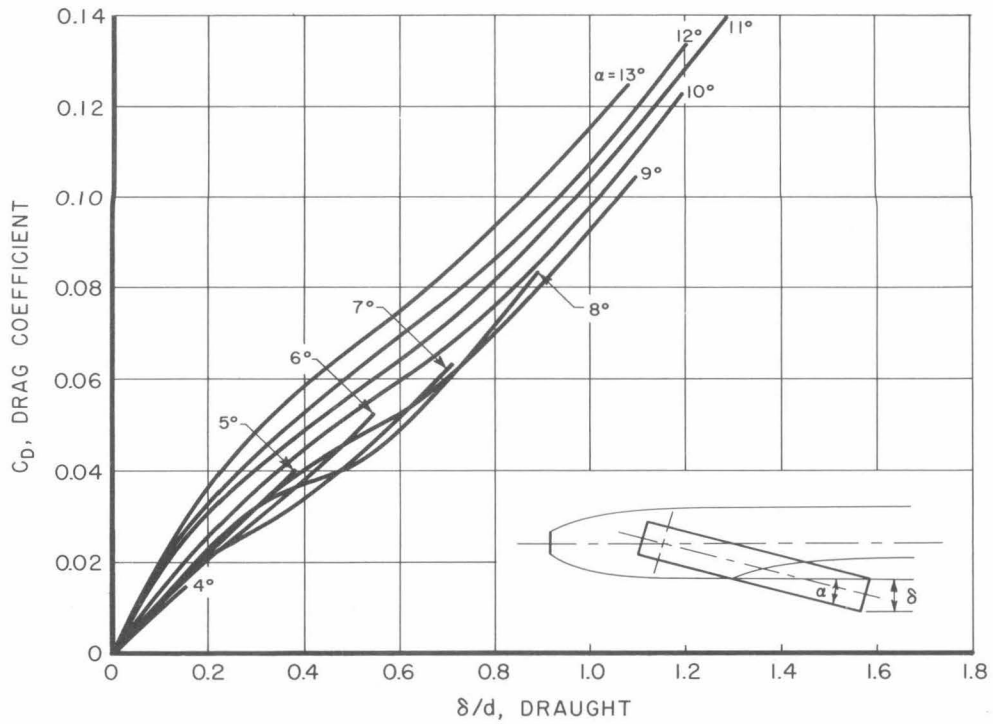


Fig. 6 - Drag coefficient vs. draught at several planing angles

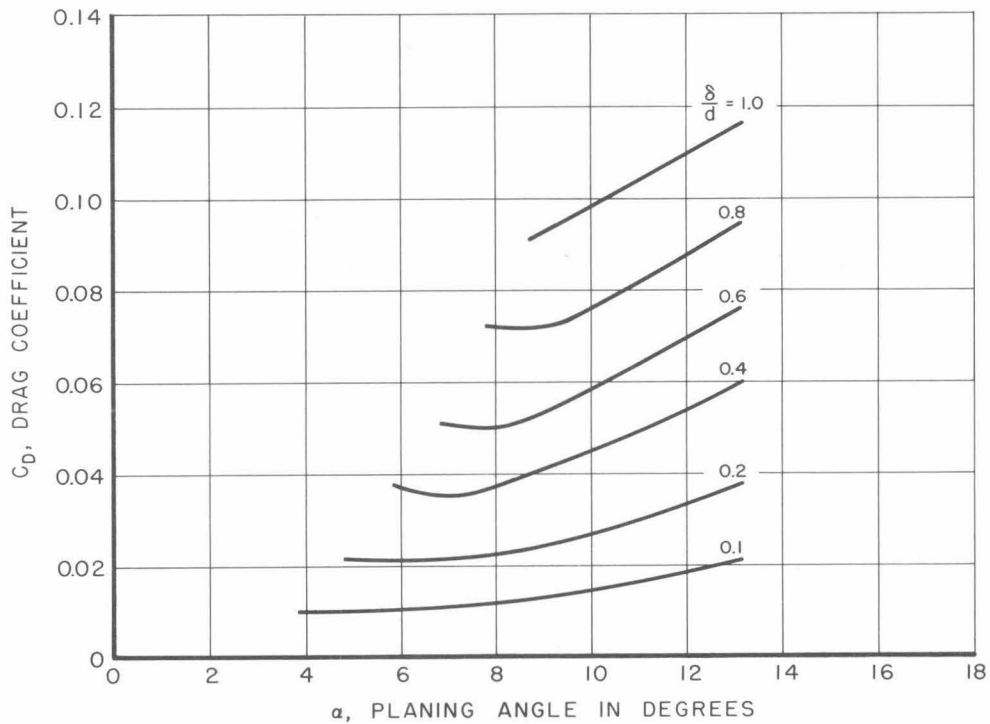


Fig. 7 - Drag coefficient vs. planing angle at several draughts

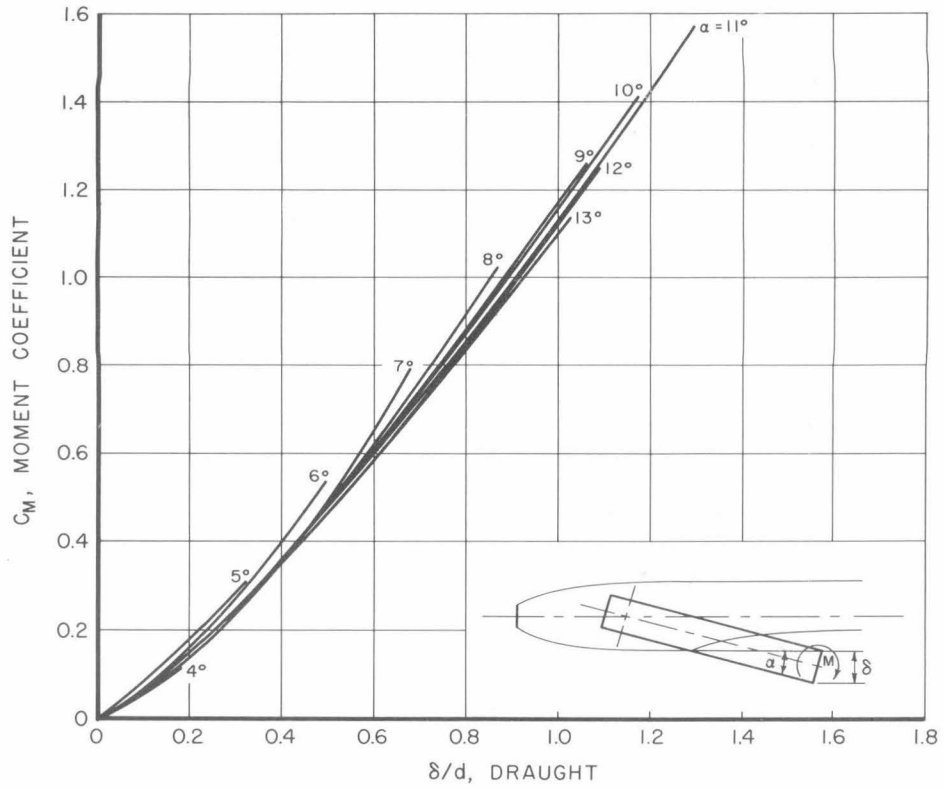


Fig. 8 - Moment coefficient vs. draught at several planing angles

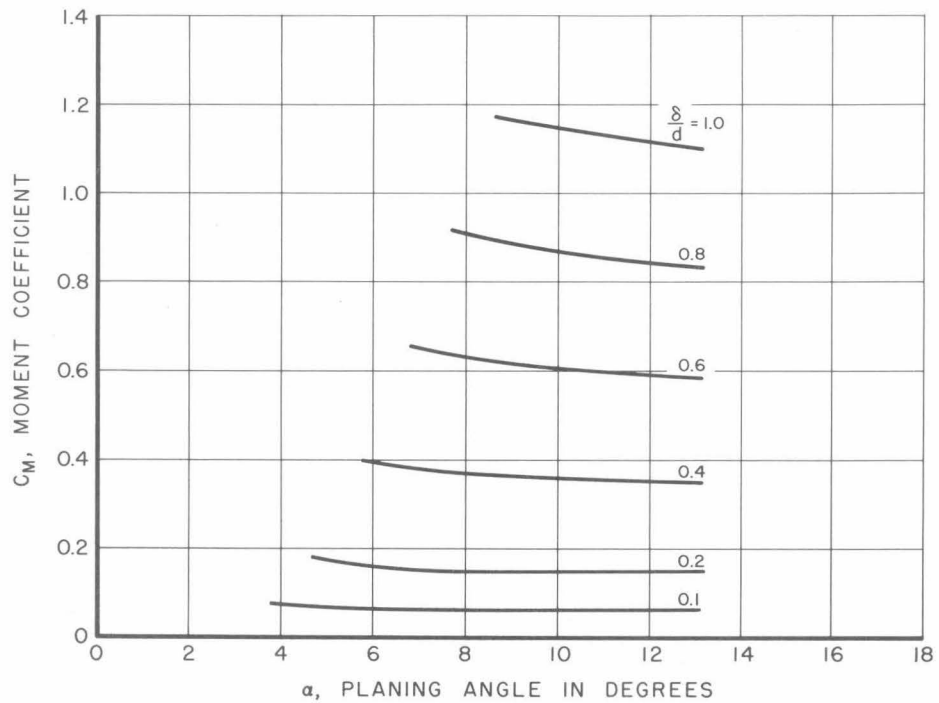


Fig. 9 - Moment coefficient vs. planing angle at several draughts

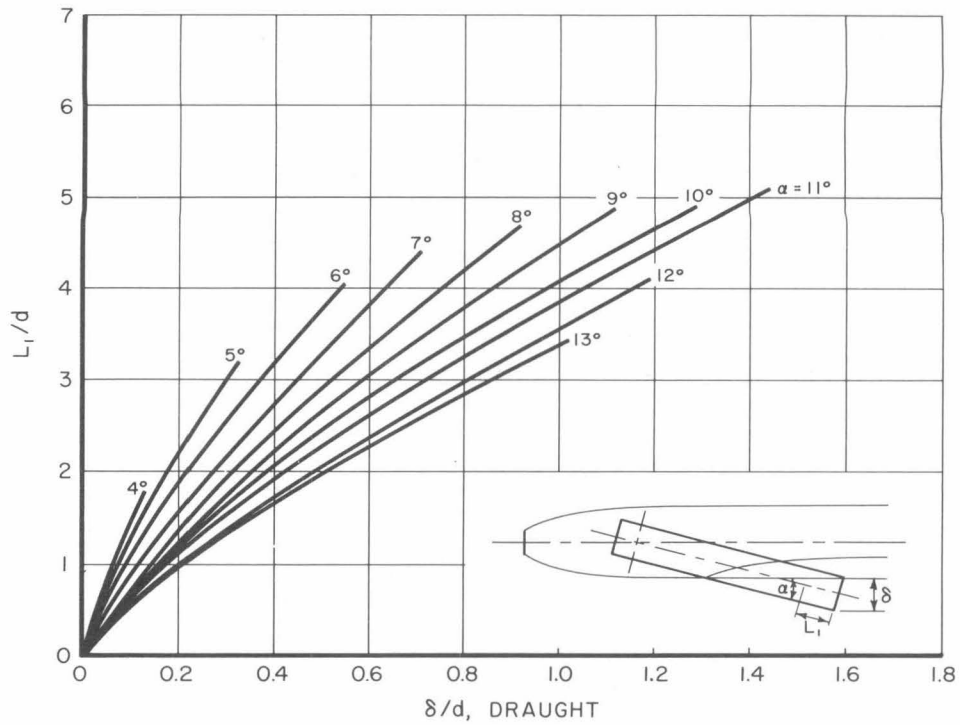


Fig. 10 - Position of center of pressure of planing cylinder vs. draught at several planing angles

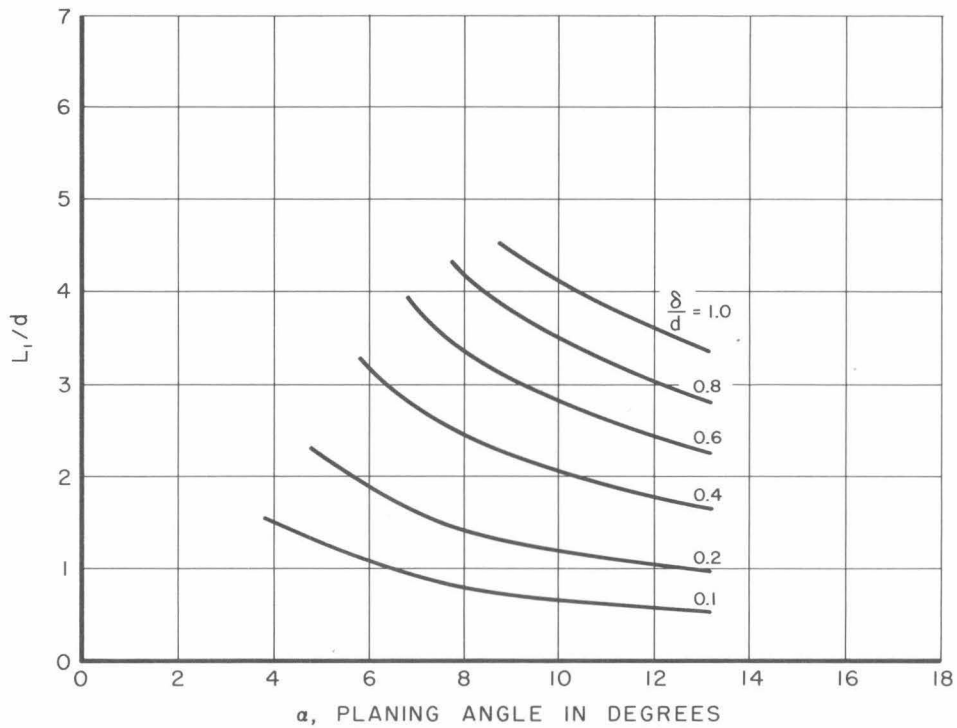


Fig. 11 - Position of center of pressure of planing cylinder vs. planing angle at several draughts

Discussion of Results

The lift coefficient curves are similar in shape to those obtained in the Free Surface Water Tunnel and by Hogg and Smith,¹ but with coefficients approximately twice as large for the same planing angle and submergence. The large differences between the lift coefficients reported here and in flat surface tests can probably be accounted for by the method of defining the draught of the cylinder. A cylinder planing through a curved cavity wall has a greater wetted surface than when planing at the same angle and draught on a flat surface. Perhaps more important is the distortion of the cavity at the intersection with the cylinder. At the point of intersection of the cylinder and the cavity wall the flow is deflected around the cylinder causing a narrowing and shortening of the cavity with a resulting large increase in the apparent draught. This apparent submergence, measured from the trailing edge of the cylinder to the wall of the distorted cavity, gives draughts approximately twice as great as those obtained when measuring submergence to the wall of the original undisturbed cavity. Use of this apparent submergence δ_1/d , defined in Fig. 3, results in lift coefficients, Figs. 12 and 13, which are much less than those plotted against δ/d in Fig. 4, but still somewhat greater than lift coefficients obtained in flat surface planing.

Additional tests will be made to investigate the effects of the ratio of cavity to planing cylinder diameter, and an attempt will be made to get a closer correlation with flat surface planing results by using a large diameter cavity and a small diameter cylinder. Future tests should also include measurements of forces on models of actual missile afterbodies.

The drag coefficients, Fig. 6, are of the same magnitude as those obtained by Hogg and Smith. The drag curves obtained in the High Speed Water Tunnel show an increase in drag coefficient with planing angle for all draughts at angles greater than 9 degrees. For angles less than 9 degrees the drag coefficient decreases slightly with increasing angle at constant draught.

The pitching moment taken about an axis through the center of the after end of the cylinder varies only slightly with changes in planing angle at constant draught, Fig. 8.

The position of the center of pressure, measured from the after end of the cylinder along the cylinder axis, changes regularly with both planing angle

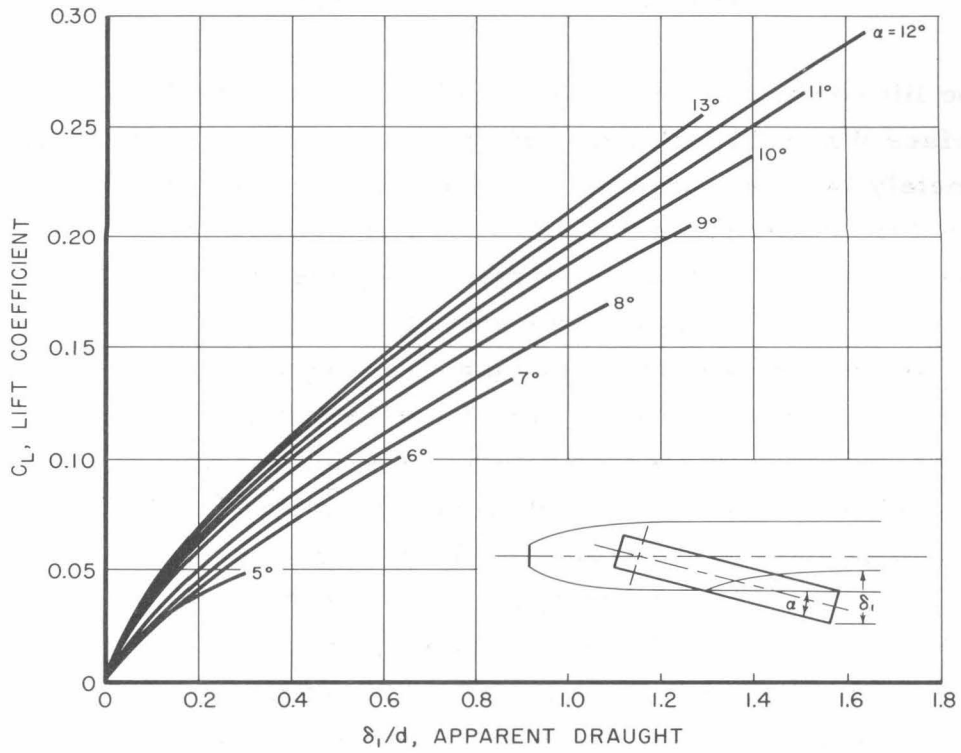


Fig. 12 - Lift coefficient vs. apparent submergence at several planing angles

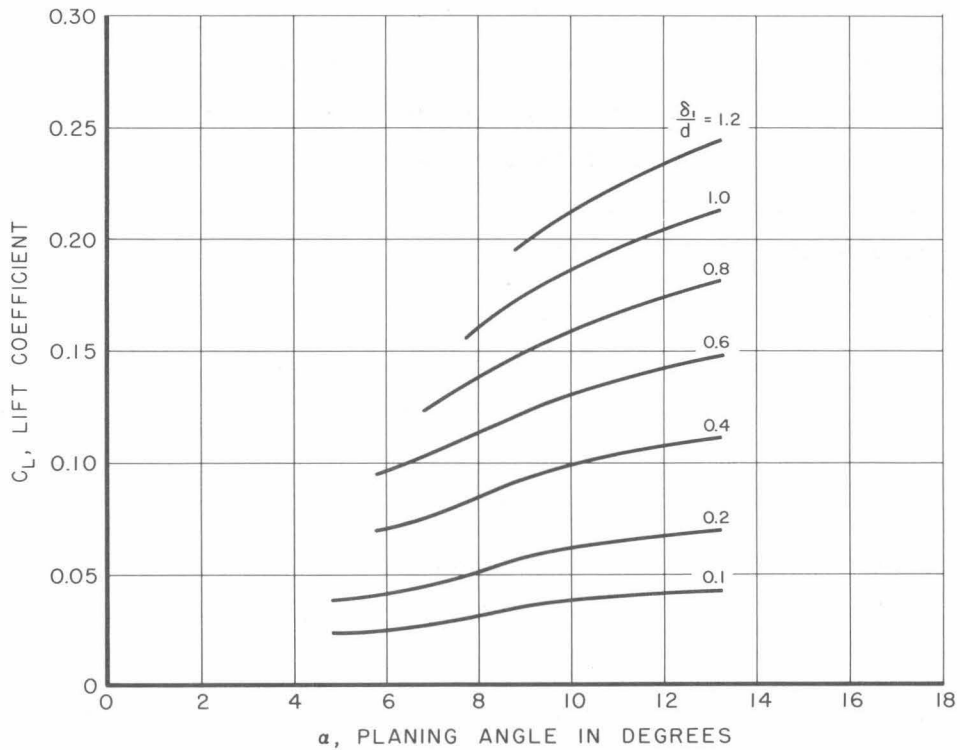


Fig. 13 - Lift coefficient vs. planing angle at several apparent submergences

and submergence. At constant planing angle the center of pressure moves forward with increasing draught, Fig. 10. This movement is much more rapid at smaller planing angles. At constant submergence the center of pressure moves aft with increasing planing angle over the entire range tested, Fig. 11.

Spray and Cylinder Cavitation

At small planing angles and depths a thin sheet of water flows along the surface of the cylinder inside the cavity and is shed off the trailing edge, Fig. 14A. At the intersection of the cylinder and cavity this sheet flows forward along the cylinder before reversing and being shed as a spray. As the angle and draught increase somewhat, the spray comes off the trailing edge of the cylinder as a complete unbroken sheet inside the cavity, Fig. 14B. For these two conditions the angle between the spray and cylinder axis increases with increasing planing angle. With further penetration of the cylinder into the cavity wall the spray sheet breaks free along the top of the cylinder, Fig. 14C. At very large draughts the water may close about the cylinder at the intersection of the cavity and cylinder and separate cavities will be formed, one from the disk and the other from the planing cylinder. In this condition spray is still shed from the cylinder inside the original cavity, Fig. 14D.

The spray sheets no doubt contribute to the forces on the cylinder; however, no correlation could be made between the spray pattern and any changes in the forces. Hogg and Smith,¹ who have described similar spray patterns in flat surface cylinder planing tests, suggest that atmospheric pressure provides the forces which cause the water film to cling to the cylinder, and that the surface tension forces are negligible. The cavity pressures measured in the High Speed Water Tunnel tests are approximately 1/25 of atmospheric pressure. This would seem to indicate that the pressure was not a significant factor in spray formation and that surface tension and viscosity forces were the determining factors.

At planing angles greater than 7 degrees and at draughts greater than half the cylinder diameter, cavitation may occur along the edge of the cylinder, Fig. 15. The cavitation along the cylinder edges may occur when there is a single cavity or when the cylinder has formed a separate cavity. For the

range of angles and draughts tested the cylinder cavitation was intermittent and no quantitative evaluation of its effects on the forces could be made. However, with cylinder cavitation there was evidence of small increases in drag with no apparent changes in the lift forces.

The Vapor Cavity

The surface through which the cylinder was planing was the wall of a vapor cavity produced behind a 1/2-in. diameter circular disk. The undisturbed cavity had an average maximum diameter of 2.15 in. and an average length of 24.04 in. The greatest variation in cavity diameter between runs was from 2.06 to 2.23 in., a difference of 8%. The average cavity diameter in the horizontal plane at the point of intersection of the trailing edge of the planing cylinder and the cavity wall was 2.10 in. Distortion of the cavity due to buoyancy was very small at 40 fps tunnel velocity and the cavity was essentially circular in cross section. The average vertical cavity diameter at the point of planing was 2.06 in, giving a distortion of only 2% in the horizontal and vertical planes. Comparative sizes of cavity and planing cylinder as well as cavity cross section shape are shown in the sketch, Fig. 3. The cylinder in all setups planed at or forward of the maximum diameter or midpoint of the cavity. Figure 16 shows top and side views of the cavity and cylinder.

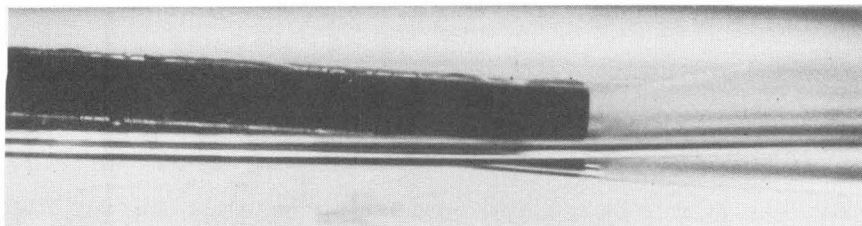
As the cylinder was yawed to increase the planing angle and draught, the closure and entrainment conditions at the after end of the cavity changed with the result that there was in general a decrease in cavity pressure, an increase in K , and a marked shortening of the cavity. Over the range of angles and draughts tested the cavity pressure decreased with increasing angle on an average of 7.5%, K increased approximately 2.5% and the cavity was shortened in some cases as much as 30%. For the low cavitation numbers used in these tests a very small change in K results in a large change in cavity length but has very little effect on cavity diameter.

Except for the preliminary runs to investigate Froude and Reynolds number effects (See Appendix A), each run was made at a constant velocity. The velocity between runs varied in the range from 39.2 to 39.8 fps. During each run the working section pressure was held as constant as possible to give a constant cavitation number and cavity size. The average cavitation number for

these tests was 0.104. With a 1/2-in. disk the minimum K obtained with a vapor cavity in the High Speed Water Tunnel is 0.090. This put a lower limit on the possible cavitation number range for vapor cavities, however, lower K's could be obtained with air-maintained cavities or smaller disks.

As noted above, the planing cylinder caused large changes in cavity size and pressure. The measured cavity pressure for the entire group of runs varied from 0.534 to 0.669 psia and K varied from 0.099 to 0.110. However, the variations in pressure and cavitation number during any one run were much less, and since the purpose of these tests was to study planing forces, no attempt was made to model cavity pressures and cavitation numbers which might exist for a prototype missile.

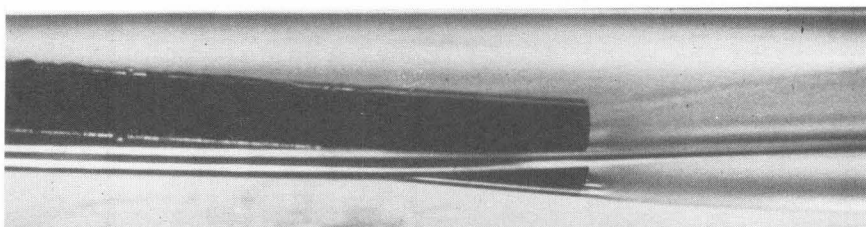
The temperature of the water in the tunnel was held between 80 and 81^oF which gave vapor pressures from 0.506 to 0.523 psi. The difference between measured cavity pressure and vapor pressure was air pressure present through diffusion across the cavity boundary and by the use of air to clear the pressure measuring lines during the runs. The air content of the water was controlled between 10.3 and 11.1 parts of air per million parts of water.



Spindle Angle

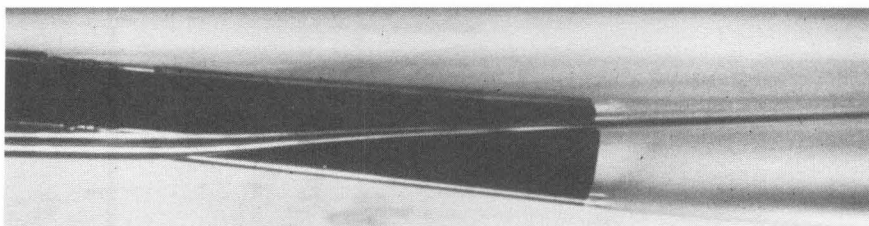
5.0°

A. Spray sheet from trailing edge



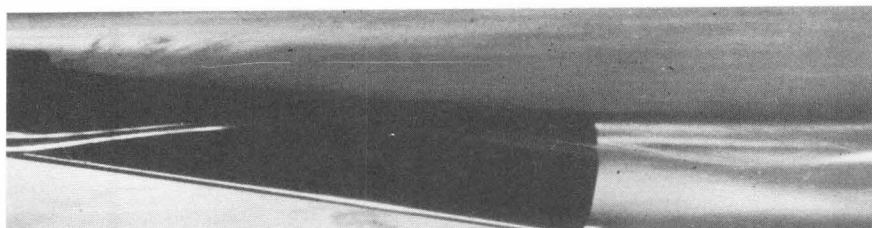
5.5°

B. Complete spray ring from trailing edge



7.5°

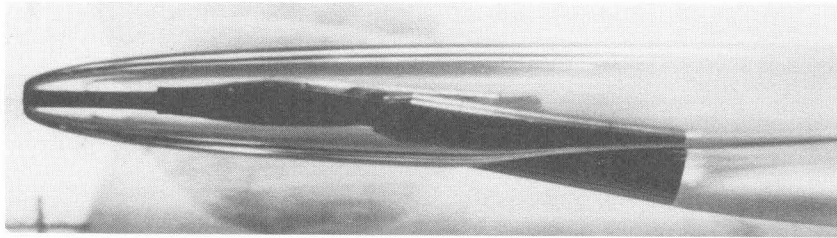
C. Spray sheet breaking clear along cylinder



10.5°

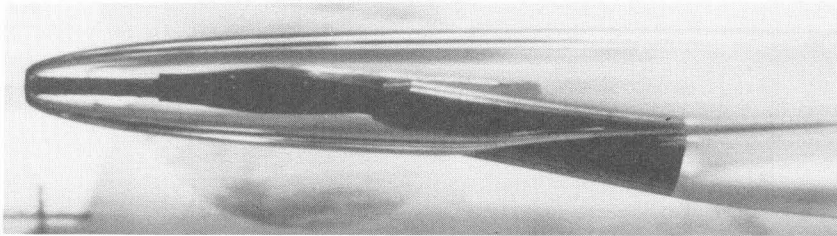
D. Separate cavity from cylinder with spray inside disk cavity

Fig. 14 - Top view of spray configurations

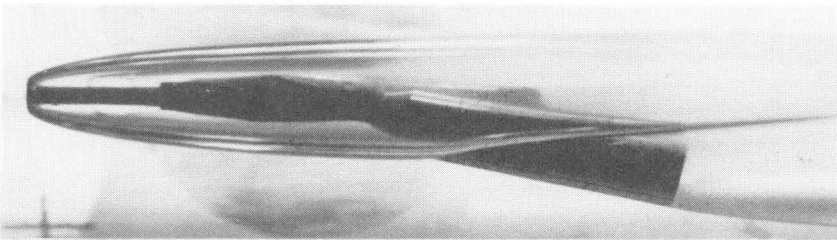


Spindle Angle

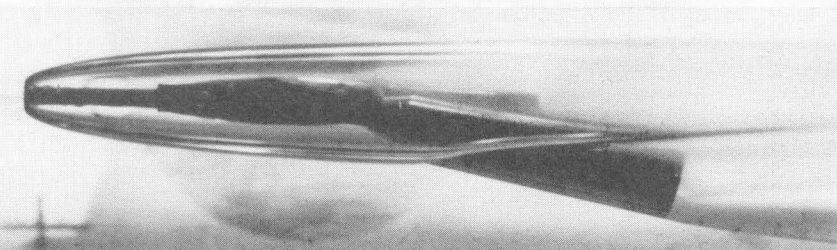
11.5°



12.0°

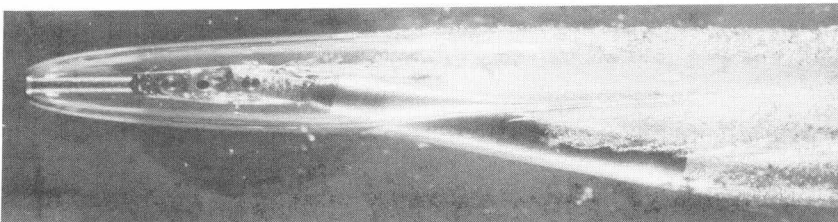


13.0°



14.0°

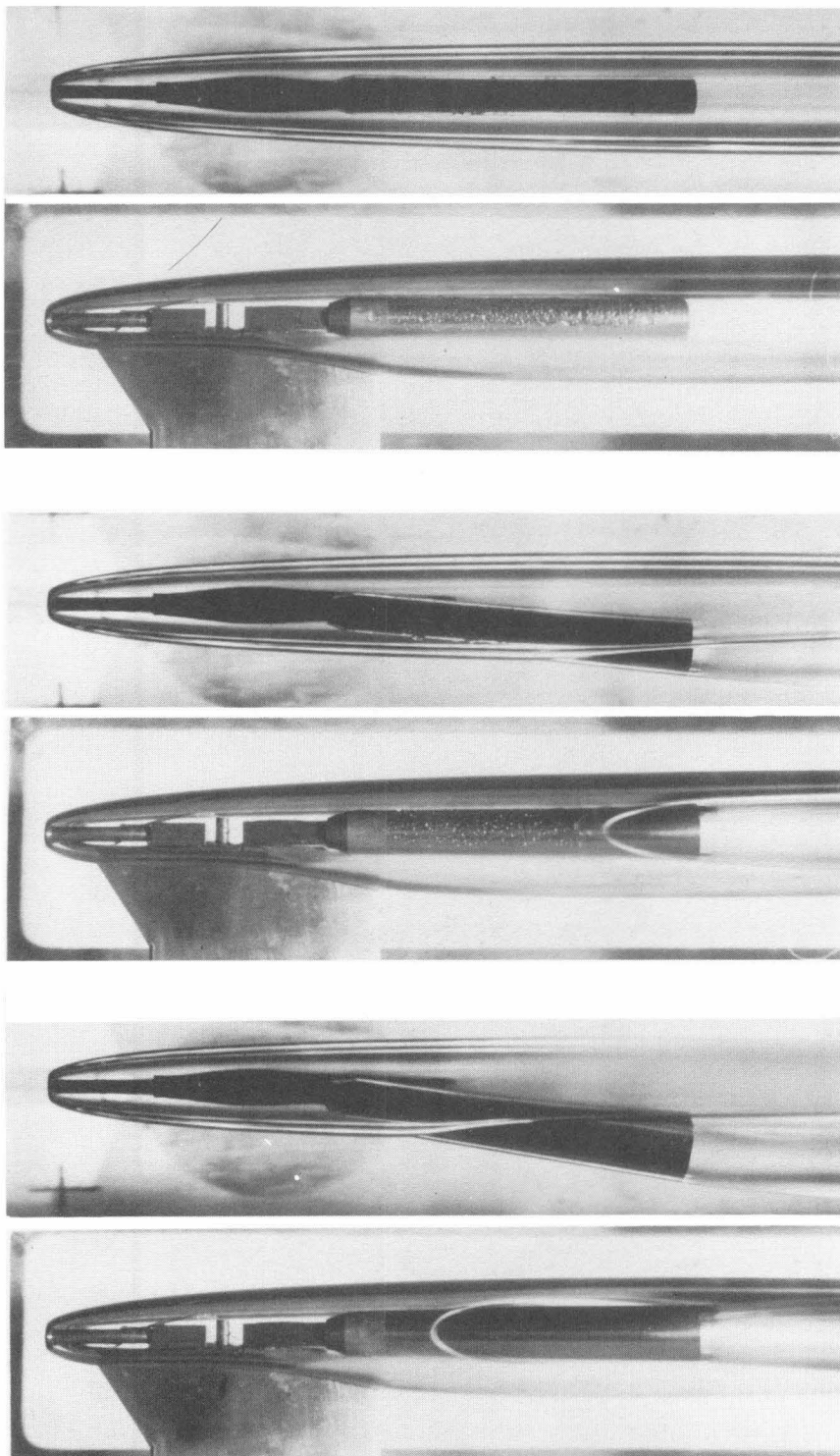
Exposure time - 1/25 second



13.0°

Exposure time - 10 microseconds

Fig. 15 - Top view of cavitation on planing cylinder



Spindle Angle

0°

7°

11°

Fig. 16 - Top and side views of cylinder planing in cavity wall

Appendix

A. Froude and Reynolds Number Effects on Force Measurements

Preliminary runs were made at water velocities of 25 to 50 fps to investigate the effects of gravitational and viscous forces on the measurements. These velocities gave a Froude number range based on cylinder diameter of from 18.0 to 30.3 and a Reynolds number range, based on cylinder diameter, of from 2.18 to 4.38×10^5 . No changes in lift coefficient with velocity were noted over this Froude number range.

An experimental investigation of the effect of Froude number on lift for a cylinder planing on a flat surface was carried out in the Free Surface Water Tunnel.² These tests included Froude numbers based on cylinder diameter up to 21 and showed little change in lift coefficient for Froude numbers greater than 18 for the planing angle and submergence range covered in the High Speed Water Tunnel tests.

There were small changes in drag coefficient at velocities less than 40 fps. Further evidence of a Reynolds number effect at low velocities was a change in the length of the clear glassy portion of the wake coming off the trailing edge of the planing cylinder at small planing angles. The length of this clear wake decreased with increasing velocity. Since these observed changes were limited to velocities of 35 fps or less, all subsequent runs were made at 40 fps.

B. Data Reduction

The forces lift, drag and pitching moment were measured directly with the water tunnel balance. The planing angle and submergence were recorded photographically. An exposure time of 1/25 second was used which gives a smooth, clear outline of the cavity and cylinder. The planing angle and submergence were measured by projecting the photographic negative with an enlarger. Using the enlarger the cavities and cylinders were superimposed and matched on the undisturbed cavity contour and the outline of the cylinder and cavity traced and planing angle and draught measured from the drawing.

The photographic method of measuring planing angle and draught made it impossible to select particular angles and draughts during the runs since the planing angle did not correspond to the balance spindle angle. Due to longitudinal curvature of the cavity, the spindle angle was from 1 to 2 degrees larger

than the planing angle. For this reason the results are presented as faired curves rather than measured data points. The curves were obtained by plotting the original force measurements and photographic data as a function of balance spindle angle, Fig. 17. This gave one set of curves for each run or cylinder length tested. From the data curves any planing angle or draught could be selected and the other information read off the remaining curves by moving vertically along lines of constant spindle angle. The method is shown by the dashed line, Fig. 17, for a planing angle of 11 degrees.

A second set of curves of force coefficients was obtained by using measured data points which were at or near selected planing angles or draughts. These curves were essentially the same as those described above and shown in this report. However, the number of data points was small using this method and the scatter relatively large due to the fact that at each angle selected, the data points necessarily covered a small range of angles on each side of the selected angle.

The pitching moment was measured about the spindle axis on the tunnel balance. The moment center defined in this report is the center of the after surface of the planing cylinder, point A, Fig. 3. The moment about point A was calculated by adding the normal components of the lift and drag force to the measured moment:

$$M_A = (\text{Drag}) L \sin \beta + (\text{Lift}) L \cos \beta - M_s$$

where:

L is the length of the cylinder and beam, Fig. 3

β is the spindle angle, Fig. 3

M_s is the measured moment about the spindle axis.

The distance to the center of pressure forward along the cylinder axis from the aft surface of the cylinder was obtained by dividing the measured moment about the spindle axis by the sum of the normal components of the lift and drag:

$$M_{CP} = (\text{Drag}) (L - L_1) \sin \beta + (\text{Lift}) (L - L_1) \cos \beta - M_s = 0$$

$$L_1 = L - \frac{M_s}{(\text{Drag}) \sin \beta + (\text{Lift}) \cos \beta}$$

where all terms are as defined above and in Fig. 3.

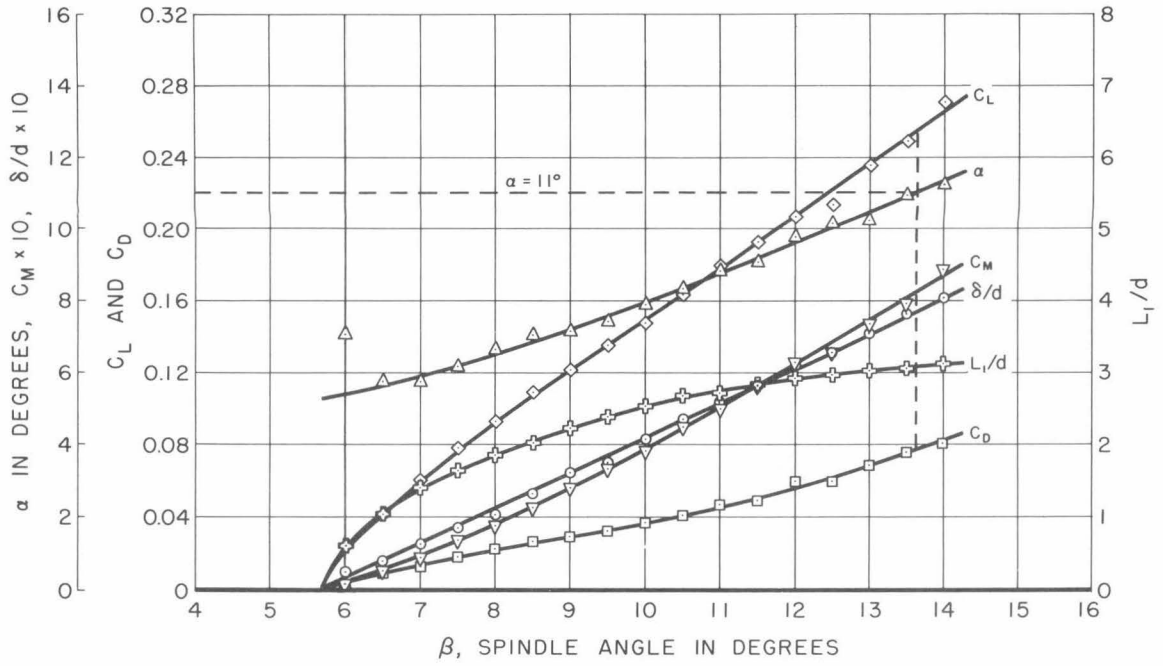


Fig. 17 - Sample data curves, Run 17

References

1. Hogg, H. and Smith, A. G., "Forces on a Long Cylinder Planing on Water", Royal Aircraft Establishment, Farnborough, England, Report No. Aero 1999, December, 1944.
2. Kiceniuk, T., "Experimental Study of Froude Number Modeling for Cylinder Planing on Water", Hydrodynamics Laboratory, California Institute of Technology, Report No. E-24.4, January, 1952. Restricted.